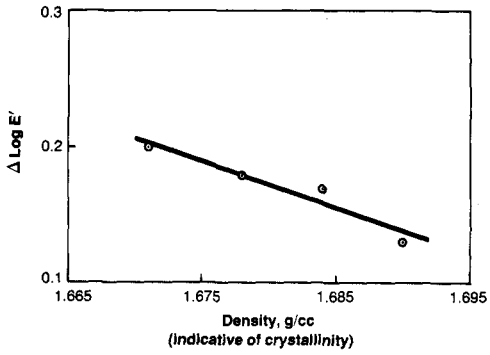

Figure 12. Change in dynamic storage modulus (Δ log E') associated with the β''-relaxation as a function of density for Halar 300.

δ curve. Quantitative evaluation of the β''-transition based on the E' data reveals that this is also an amorphous phenomenon (Figure 12). It is known that many polymers exhibit a β-transition below the T_g at a temperature such that $T_\beta/T_g \simeq 0.75$.[10] Also it has been suggested that the β-peak at $0.75T_g$ represents the motions of short amorphous segments. Considering the β'-relaxation as the T_g of Halar, the ratio β''/T_g is about 0.83. Therefore, we believe that the β''-relaxation involves the small-scale or local motion of the amorphous segments of Halar.

To conclude our view on the β-relaxation(s) in Halar, we propose that the β'-peak at 85 ± 5 °C is the T_g of Halar whereas the β''-peak at 50 ± 5 °C is due to the motion of short amorphous segments. Activation energies of 107 and 66 kcal/mol for the β'- and β''-relaxations, respectively, support that these represent large- and small-scale motions of the amorphous regions.

γ-Relaxation. The γ-peak occurs as a very broad peak extending from −120 to +20 C, with the maximum at about −55 °C (Figure 3 and Table II). Its peak intensity remains more or less unaffected by the crystalline (or amorphous) content (Table II).

The lowest temperature relaxations in mechanical spectra have generally been attributed to the motions of the small units of the polymer chain, perhaps 3–4 carbon atoms in length.[5,10,11] The small units in Halar responsible for the α-peak probably comprise (a) short blocks of ethylene (CH_2), (b) short blocks of chlorotrifluoroethylene ($CClFCF_2$), (c) short segments of amorphous 1/1 alternating copolymer, i.e., Halar, and (d) loose chain ends within the amorphous and crystalline phases of Halar. A range of physicochemical environments of the units involved is most likely responsible for the extreme broadness of the γ-relaxation. Comparatively, a low value of the activation energy of the γ-peak (27 kcal/mol) is in agreement with the assignment that it is related to the motions of very small units of the polymer.

Acknowledgment. We thank Mrs. A. Reimschuessel and Prof. S. Krimm for helpful comments and suggestions. Also we acknowledge the contributions of T. Taylor and the late D. Richardson for thermal analysis, S. Murthy, A. Szollosi, and H. Minor for X-ray diffraction, N. Buik for density measurements, and F. Cilurso for viscosity data. We also thank B. Buckner for his high-quality mold-processing work.

Registry No. Halar, 25101-45-5; (E)·(CTFE)·(HFIB) (copolymer), 67124-01-0.

References and Notes

(1) Khanna, Y. P.; Turi, E. A.; Sibilia, J. P.; Sacks, W. *J. Appl. Polym. Sci.* **1984**, *29*, 3607.
(2) Khanna, Y. P.; Turi, E. A.; Sibilia, J. P. *J. Polym. Sci., Polym. Phys. Ed.* **1984**, *22*, 2175.
(3) Sibilia, J. P.; Schaffhauser, R. J.; Roldan, L. G. *J. Polym. Sci., Polym. Phys. Ed.* **1976**, *14*, 1021.
(4) Starkweather, H. W., Jr. *J. Polym. Sci., Polym. Phys. Ed.* **1973**, *11*, 587.
(5) Khanna, Y. P.; Turi, E. A.; Taylor, T. J.; Vickroy, V. V.; Abbott, R. F. *Macromolecules* **1985**, *18*, 1302.
(6) Boyd, R. H. *Polymer* **1985**, *26*, 323.
(7) Sibilia, J. P.; Roldan, L. G.; Chandrasekaran *J. Polym. Sci., Polym. Phys. Ed.* **1972**, *10*(3), 549.
(8) Starkweather, H. W., Jr. *Macromolecules* **1981**, *14*, 1277.
(9) Rabolt, J. F. *Polymer* **1981**, *22*, 890.
(10) McCrum, N. G. In *Molecular Basis of Transitions and Relaxations*; Meier, D. J., Ed.; Gordon and Breach: New York, 1978.
(11) Khanna, Y. P. *J. Therm. Anal.* **1985**, *30*, 153.

Field-Induced Textures and Elastic Constants of Nematic Polymers†

Curtis R. Fincher, Jr.

Central Research and Development Department, Experimental Station, E. I. du Pont de Nemours and Company, Wilmington, Delaware 19898. *Received February 19, 1986*

ABSTRACT: Studies of the development of periodic textures or patterns in a nematic liquid crystalline polymer when a magnetic field is applied orthogonal to the director of the sample are presented. The strong anisotropy of the light scattering from this polymer allows for a clear definition of the obtained texture. While the patterns can be explained by earlier theories for small-molecule nematics, one must assume the existence of a strongly anchored director, contrary to fact.

In recent years there has been considerable effort spent in the investigation of the physics of liquid crystals and more recently an expanding effort in polymers. These two fields share not only many analogies but also a whole class of materials commonly referred to as liquid crystalline polymers (LCP's).[1] LCP's are commonly found in biological systems (generally cholesteric) but have also been found to be technologically important in terms of high-performance materials.[2] In spite of the driving forces of science and technology many of the fundamental properties of these materials are relatively unexplored. The problems have not been due to a lack of interest but rather because many of the standard approaches and techniques which have been developed during the extensive work on small-molecule nematics experience difficulties when applied to investigations of polymeric nematics. As an example, to make most measurements on a nematic mean-

† Contribution No. 3731.

0024-9297/86/2219-2431$01.50/0

ingful it is necessary to have well-defined boundary conditions for the director. These boundary conditions are generally obtained by use of suitable surface treatments as to obtain so-called "strong anchoring" at the sample surfaces (i.e., the energy for changing the orientation of the director at the surface is so much larger than any other energy scale in the problem that one assumes a fixed boundary condition).[3] Well-defined boundary conditions have been difficult to obtain for the polymeric materials and as a result the investigations have been hindered.[4]

In earlier work by Guyon et al.[5] and Lonberg et al.,[6] it was shown how that in an aligned monodomain sample of a liquid crystal such as *N*-(*p*-methoxybenzylidene)-*p*-butylaniline (MBBA), the system develops a periodic structure in response to a magnetic field applied normal to the original direction of the director orientation. The structure is a result of the system propagating from the ordering ground state to a newly defined ground state via a higher energy metastable state. The mechanism for the wave vector selection was analyzed and found to agree with measurements of the phenomena in MBBA. The theory considers the time evolution of a periodic fluctuation of the director in the sample. The sample is a thin slab of liquid crystal of thickness d, with the plane of the slab in the x–z plane and the director parallel to the z axis. If we use $\Theta(x,y,z)$ to describe the angle the director makes with the z axis and the director n is confined to the x–z plane, the director may be described by the single variable Θ.

$$\hat{n} = \hat{x} \sin \Theta + \hat{z} \cos \Theta \tag{1}$$

A fluctuation of the director can now be described by the spatial and time dependence of Θ. The theory assumes a fluctuation of the form

$$\Theta(x,y,z,t) = \Theta_0(t) \cos (k_x z) \sin (k_y y) \tag{2}$$

$$k_y = \pi/d$$

It further assumes that the time dependence of $\Theta_0(t)$ has a relatively simple form such as

$$\Theta_0(t) = \Theta_{00} \exp(st) \tag{3}$$

The exponent s will in general have a wave vector dependence while the sign of s determines whether the fluctuation grows ($s > 0$) or decays ($s < 0$) with time. The selection mechanism results from the exponent exhibiting a well-defined maximum with respect to the wave vector. At this wavelength, for which s is a maximum, the growth rate is exponentially larger than at other wavelengths. Because this theory is a linearized version of the true time dependence, only the early-time behavior can be accurately described. Once the process begins, the nonlinearities will rapidly become nonnegligible, with the result that the problem becomes intractable. In spite of this, the configuration of the director at long times is conceptually easy to visualize and understand. It is the result of an arrangement of cells with a spacing determined by the above mechanism. Each cell separated by domain walls is created by an alternating sense of rotating flow. The flow ceases when the elastic energy is balanced by the magnetic energy leaving the sample in a metastable state that at much longer time scales evolves into the true ground state by the elimination of the domain walls.

Experimental Section

The samples used in this experiment were thin (25–1000 μm) slabs of poly(1,4-benzamide) (PBA) captured between two glass plates separated by a polymer spacer. The samples were prepared by using either of two solvents. The first solvent used was dimethylacetamide with 5% by weight LiCl as described by Panar and Beste.[7] Samples were also prepared by using 100% sulfuric acid. In order to be able to compare different molecular weights in some standard fashion the samples were made at a concentration c^*, the lowest concentration above the biphasic range of concentrations. For a sample of $[\eta] = 1.18$ dL/g or a molecular weight of about $M_w = 1.7 \times 10^4$, c^* corresponds to a concentration of approximately 20% by weight to volume. In order to ensure the absence of any isotropic fraction, the material was centrifuged well past the time that examination by a microscope failed to reveal any remaining isotropic material in the sample. After preparation the samples were placed in a magnetic field of 8–10 kOe with the field in the plane of the thin dimension of the sample. The high field and large magnetic anisotropy cause the sample to relax into a highly ordered monodomain with the director along the field. After this initial period the sample is turned about the vertical axis by 90° so that the field is now applied normal to the director. The various textures that resulted from the reorientation in this second applied field were the object of this study.

Results

After placing the material in an external magnetic field, we first observed the anisotropy of light scattered at 90° for light propagating along or transverse to the applied magnetic field. Defining the quantity $I_\parallel$ as the light scattered with the propagation vector $\vec{k}$ parallel to the director and $I_\perp$ as the scattered light for $\vec{k}$ perpendicular to the director, we measured the anisotropy factor

$$A = (I_\perp - I_\parallel)/(I_\perp + I_\parallel) \tag{4}$$

This anisotropy of the scattering grows from zero to approximately 0.5 after the application of the magnetic field. While the data are not a completely accurate measurement of the scattered intensity due to multiple-scattering effects, the observed relaxation to a steady state does demonstrate that the scattering cross section for $\vec{k}$ parallel to $\hat{n}$ is significantly less than for light propagating normal to the director. In addition one finds that the time for orientation depends strongly upon molecular weight, increasing by roughly a factor of 100 for $0.72 < [\eta] < 1.67$ dL/g and is relatively unaffected by the solvent used. Striking textures are obtained after the application of the second magnetic field orthogonal to the director orientation. The actual time required for the development of the textures varies from 20 s to 24 h, depending upon the molecular weight and magnitude of the applied field. One observes the formation of thin dark lines with a highly regular spacing running parallel to the applied field. An additional interesting effect is noticed if one uses light which is obliquely incident. When the incident light has a component in the plane of the sample, the regions between the dark lines appear alternately bright and dark. This effect is illustrated in Figure 1 for several values of the magnetic field. The contrast between the bright and dark areas of the liquid is maximized when the projection of $\vec{k}$ into the plant of the sample is at an angle of 45° with respect to the set of thin dark parallel lines. If this angle is changed by 90° then the formerly bright regions of liquid are observed to appear dark while those formerly dark areas appear bright to inspection. The spacing of this periodic structure is found to depend upon the applied magnetic field. A measurement of the field dependence for a sample of $[\eta] = 1.18$ dL/g in DMAC/LiCl is presented in Figure 2. The data presented are for a series of solutions prepared at different dates and of different thicknesses. As the applied field is reduced the spacing grows larger (smaller wave vectors) and the time required for the development of the texture becomes longer. Finally one reaches fields for which one does not observe pattern formation. Obviously because of the increasing time scale, this boundary can not be absolute. Since the data appear to asymptotically approach a horizontal line, one can rather clearly identify a value for a critical field which is the

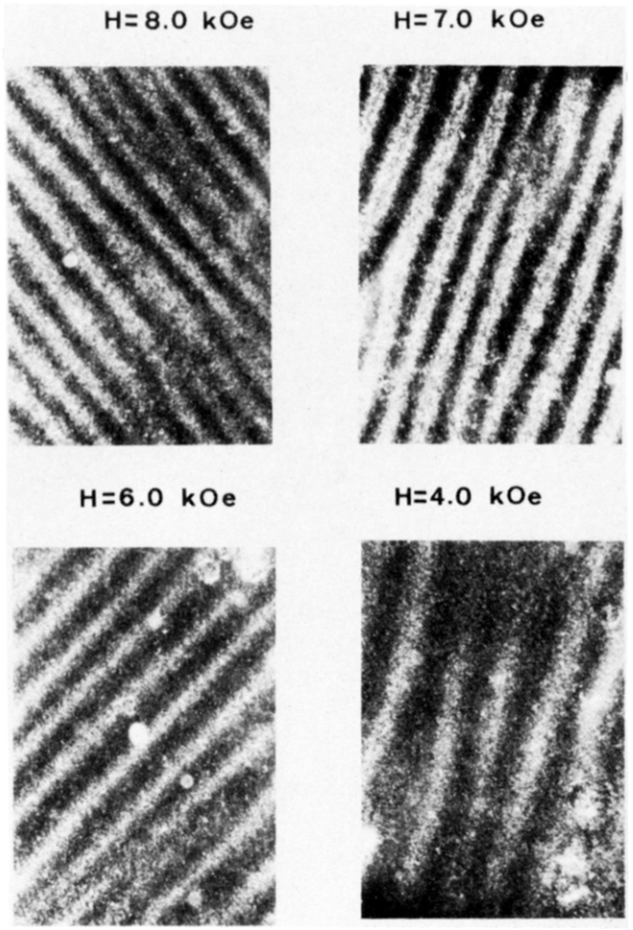

Figure 1. Examples of the periodic texture that develops when the nematic polymer is reoriented by a magnetic field orthogonal to the director. In all cases the magnetic field was applied along the direction of the bands. The photographs were taken with samples rotated by different angles maximizing the visual contrast.

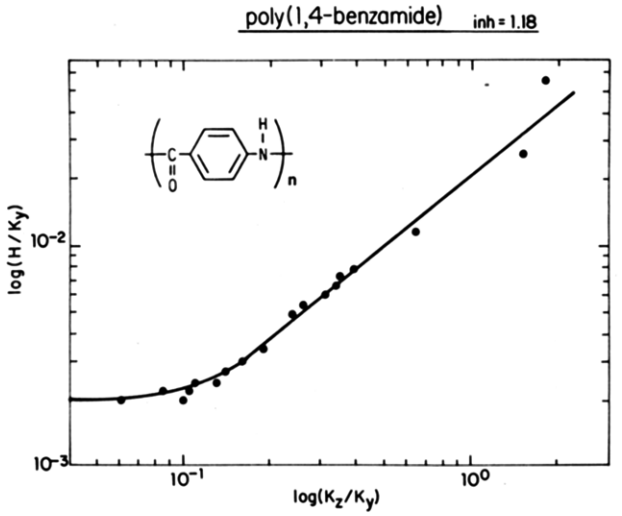

Figure 2. Magnetic field dependence of the observed wave vector for a sample of PBA with $[\eta] = 1.18$ dL/g. Both the wave vector and the magnetic field are scaled by the thickness of the sample.

smallest possible field for which pattern formation is observable. In the case of the data presented in Figure 2, it gives a value for the scaled critical field of

$$H_c(d/2\pi) = 2.1 \times 10^{-2} \text{ kOe-cm} \quad (5)$$

Discussion

These observations lead one to build an intuitive picture of the process, which is depicted in Figure 3. The original

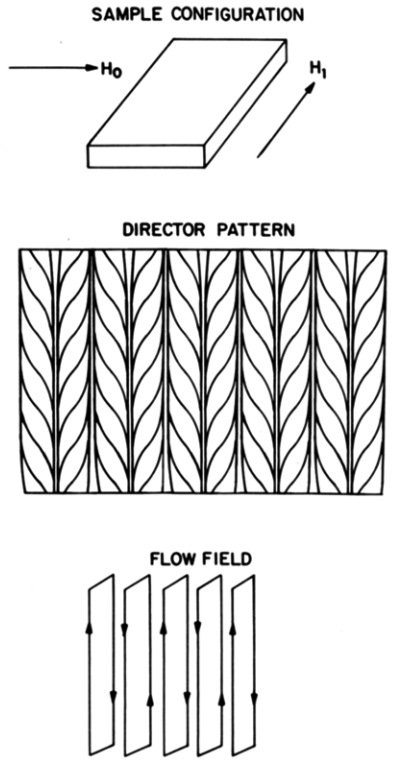

Figure 3. The top portion of the figure indicates the geometry used in the experiment. First the material is oriented by H_0, and at a later time the transverse field H_1 is applied. The middle part of the figure is a schematic representation of the herringbone-like director texture observed. Light propagating along the director in one cell is then normal to the director in the next cell, resulting in a strong modulation of the scattered intensity.

direction of orientation of the director in the sample is along the horizontal of the figure parallel to the applied field, H_0. The second field, H_1, is applied in the vertical direction of the figure. As the sample attempts to adjust to the new field, fluid flow is induced parallel to the direction of the second field. The cell-like character of the flow is indicated at the bottom of the figure. This flow pattern results in a director texture, shown schematically in the central portion of the figure. Note how the result is a series of regions resembling something like a herringbone structure. This texture gives rise to the alternating bright and dark areas of Figure 1 when light propagates in the plane of the figure but at an angle of about 45° with respect to the vertical. The disinclination-like structure, which serves as the boundaries between these regions, results in the series of dark lines in the sample. The solid line in Figure 2 represents a best fit to the data of the form

$$H = H^*[1 + Ax^2 + Bx^4] \quad (6)$$

$$x = k_z/k_y$$

This is the same form as used by Ionberg et al.[6] to describe their data for MBBA. In order to gain some understanding of these parameters it is necessary to review the form of the function used to describe the data. The exponent s in eq 2 is shown in ref 3 to have the form

$$s(k_z) = \frac{\chi_A H^2 - K_2 k_y^2 - K_3 k_z^2}{\gamma_1 - \alpha_2^2/[\eta_c + \eta_a(k_y/k_z)]^2} \quad (7)$$

where we have defined the magnetic anisotropy as $\chi_A = \chi_\parallel - \chi_\perp$. Solving eq 6 for the wave vector where the exponent $s(k_z)$ exhibits a maximum will give the functional

relation between the applied magnetic field and the wavelength of the observed pattern. We find

$$\left(\frac{H}{H_c}\right)^2 = 1 + \left(\frac{K_3}{K_2}\right)\left(\frac{\gamma_1\eta_a}{\alpha_2{}^2}\right) + \left(\frac{K_3}{K_2}\right)\left(\frac{2\gamma_1\eta_a}{\alpha_2{}^2}\right)\left(\frac{\eta_c}{\eta_a}\right)x^2 + \left(\frac{K_3}{K_2}\right)\left[\left(\frac{\gamma_1\eta_a}{\alpha_2{}^2}\right)\left(\frac{\eta_c}{\eta_a}\right)^2\left(\frac{\eta_c}{\eta_a}\right)\right]x_4 \quad (8)$$

where K_n's represent the Frank elastic constants while α_i, γ_i, and η_i are viscosity coefficients. All the parameters used are those standard to the Leslie–Eriksen–Parodi formulation of nematodynamics.[3] Interestingly, the scaled critical field, $H_c d/2\pi$, remains relatively constant for all three molecular weights (for $M_w = 2.3 \times 10^4$, $H_c = 2.7 \times 10^{-2}$ kOe-cm and for $M_w = 1.1 \times 10^4$, $H_c = 2.4 \times 10^{-2}$ kOe-cm), while the other parameters vary quite widely. The large variation of the other parameters along with the complexity shown in eq 6 results in a loss of information content for these parameters.

One should note that according to eq 6 if all data are scaled properly for the sample thickness, then the results of different samples can be plotted together. This was exactly the procedure followed to produce Figure 3 with the exception that for each thickness data at the highest obtainable fields were not plotted because the scaling relation appeared to fail. At the highest fields data points tended to fall above the shown curve, appearing to approach some saturation value. It is probably more surprising that the data can be described by the theory for even some limited range than that there are clear deviations away from the theory. One should first note that the presented functional relation for the wave vector dependence upon magnetic field was derived by assuming strong anchoring at both glass surfaces. This is clearly not the case for our samples. While the glass substrates used in this work were scrupulously cleaned before use, there was never any attempt made to introduce any anisotropy in the plane of the substrate itself. It is also highly unlikely that there could be any natural anisotropy in the glass used since the orientation with respect to the magnetic field was random. Since there are clear indications that the polymer does prefer a planar orientation when confined between glass plates, the probable configuration of the system is one of randomly oriented regions with the director in the plane of the glass substrate. Only after the application of a magnetic field is the sample in a monodomain configuration. There have been experiments by Hui et al.[9] on a different lyotropic system in which there were no anchoring conditions. These workers adapted the description of Lonberg et al. to apply to free rotation at the glass boundaries. In this case a completely different relation between the wave vector and magnetic field was found. Hui et al.[9] found that when the director was free to rotate at the surface, the wave vector was simply linearly related to the magnetic field. This appeared to be in excellent agreement with their observations for disodium cromoglycate in water. Figure 2 clearly shows that PBA does not exhibit a simple linear relation between the wave vector and the magnetic field. The most likely explanation is that in this case the director can choose any direction in the plane but that there is a significant hindrance to reorientation at the surface. This can be thought of as a strong viscous force at the surface which leads to boundary conditions which should be similar to the standard "no-slip" conditions used in hydrodynamics. Although solution of the differential equations describing a viscous force at the boundary proves to be extremely difficult, one can build an intuitive picture of the processes involved. At early times the highly viscous interaction at the surface means that the majority of the fluid responds much faster than the director near the surface. Because the pattern is basically a result of the instability at early times, one obtains a result much like the case of strong anchoring. There are clearly observable differences between the behavior of these samples and the results on MBBA reported by Lonberg et al.[6] As examples are the deviation of the data from the theoretical curve at high fields and that the periodic texture relaxes back to the original uniform state only if it is removed from the field soon after the pattern is apparent.

It is very interesting that the data for the three molecular weights show little or no variation in the first coefficient. as stated this coefficient is a complicated combination of several intrinsic parameters of the liquid. While it is difficult to guess how the elastic constants might change with molecular weight, measurements on these samples show that the viscosities vary greatly. If one were to use the simple experiment described above measuring the time for development of the anisotropy of the light scattering cross section, then the characteristic time for reorientation varies by more than 2 orders of magnitude for this set of samples. One finds it difficult to believe that the other material parameters would conspire to vary in such a way as to just cancel any effect of molecular weight. In fact most indications are that while the effect of molecular weight is relatively small for some of the elastic constants and viscosity coefficients, the effect is very large for others.[3] In particular the rotational viscosity γ_1 and the viscosity coefficient α_2 are expected to diverge as one approaches infinite molecular weight. This suggests a second possible explanation of these curious results. If γ_1 and α_2 grow as some power of the rod length or molecular weight, then the correction to the second term of eq 7 will vary inversely with molecular weight. In this case it is then possible that the molecular weight dependence might be too small to be measurable. This might then explain why the asymptotic value of H at small values of reduced wave vector is independent of the molecular weight in this experiment. The value might then be taken to be representative of the critical field measuring the twist elastic constant in terms the anisotropy of the magnetic susceptibility. Previous measurements of the magnetic anisotropy report values of about the same as benzene.[10] Using this value we estimate the twist coefficient of about $K_2 = 0.86 \times 10^{-6}$ dyn. This value is entirely consistent with typical values for monomeric liquid crystals.

It is curious that the material properties of nematic polymers are not well characterized. Although the small-molecule liquid crystals the properties are much more controlled by the local chemical structure, their study has provided many insights into the general features of nematic liquids. In the case of nematic polymers with the ability to vary either chain stiffness or molecular weight, it may be possible to separate general features of nematic liquids from those connected to specific structure. Furthermore, one may hope that a deeper knowledge of the nematic polymers may provide insight into the properties of other polymer systems that do exhibit mesophases. While the fluid dynamics of nematic liquids is well described by several theories, the fluid behavior of polymeric liquids is far from understood.[11,12] The results of this work show that the theories for small-molecule nematic systems apply as well to polymeric liquids in the nematic state.

Therefore, since one may think of proceeding to normal polymers by increasing the chain flexibility, the point of crossover between nematodynamics and conventional polymer rheology in these rigid polymer systems could give important clues to a fundamental understanding of polymer rheology.

Registry No. PBA (homopolymer), 25136-77-0; PBA (SRU), 24991-08-0.

References and Notes

(1) Ciferri, A. In *Polymer Liquid Crystals*; Ciferri, A., Krigbaum, R., Myer, R. B., Eds.; Academic: New York, 1982.
(2) Prevorsek, D. C. In *Polymer Liquid Crystals*; Ciferri, A., Krigbaum, R., Meyer, R. B., Eds; Academic: New York, 1982.
(3) de Gennes, P. G. *The Physics of Liquid Crystals*; Oxford, London, 1975.
(4) Taratuta, V. G.; Hurd, A. J.; Meyer, R. B. *Phys. Rev. Lett.* **1985**, *55*, 246.
(5) Guyon, E.; Meyer, R. B.; Salam, J. *Mol. Cryst. Liq. Cryst.* **1979**, *54*, 261.
(6) Lonberg, F.; Fraden, S.; Hurd, A. J.; Meyer, R. B. *Phys. Rev. Lett.* **1984**, *52*, 1903.
(7) Panar, M.; Beste, L. F. *Macromolecules* **1977**, *10*, 1401.
(8) Flory, P. J., *Proc. R. Soc. London, Ser. A* **1956**, *A234*, 73.
(9) Hui, Y.; Kuzman, M. R.; San Miguel, M.; Labes, M. M. *J. Chem. Phys.* **1985**, *83*, 288.
(10) Tsevtkov, V. N. *Liquid Crystalline Order in Polymers*; Blumstein, A., Ed.; Academic: New York, 1978.
(11) Bird, R. B.; Armstrong, R. C.; Hassager, O. *Dynamics of Polymeric Liquids*; Wiley: New York, 1977; Vol. 1.
(12) Lodge, A. S. *Elastic Liquids*; Academic: New York, 1964.

Mechanism of Polymer-Supported Phase-Transfer Catalysis. Effect of Phase Ratios on Low Percent Ring Substitution Microporous Polystyrene Resin

Susan Telford, Paul Schlunt, and Pao C. Chau*

Department of AMES (Chemical Engineering), University of California, San Diego, California 92093.

Received January 2, 1986

ABSTRACT: The liquid-phase ratio was shown to have significant effect on the kinetics of the displacement reaction between 1-bromooctane and potassium cyanide by polystyrene-bound tri-*n*-butylphosphonium ion. It was illustrated that the organic phase must be the dispersed phase to carry out the reaction effectively with microporous, low cross-linked density and low percent ring substitution polystyrene chloromethylated resins. Drastic kinetic rate improvement was achieved with proper adjustment of phase ratios and the amount of catalyst for a given organic phase volume. The mechanism was explained with an alternating-shell model.

Introduction

The catalytic activities of polymer-supported phase-transfer catalysts often are much lower than those of their homogeneous analogues, and it is generally agreed that diffusional resistance within the polymer particle is an important factor.[1] Many of these discussions on mass-transfer limitations are based on seven basic steps of modeling heterogeneous catalysis: (1) transport of limiting reactant to particle surface, (2) diffusion of reactant into particle, (3) adsorption of reactant on active site, (4) chemical reaction, (5) desorption of product, (6) counter-diffusion of product out of particle, and (7) transport of product away from particle. These physicochemical processes in this model all refer to a single limiting reactant in one fluid phase. In earlier developments, a model assuming the existence of inverted micelles within the polymer matrix was proposed to explain the microenvironment of the catalysts.[2] Kinetic data also have been analyzed with a model assuming that the diffusion of the organic reactant is the rate-limiting step.[3] More recent attempts have illustrated that the mechanism is very different with low or high percent ring substitution polymer supports.[2,4] With low percent ring substitution, the ion transport in the ion-exchange process is the rate-limiting step.[4] External mass transport of the reactant to the particle surface is regarded as not important if the reactor is vigorously agitated, usually above 600–700 rpm with a stir bar or an impeller.

Our present effort attempts to elucidate the reaction mechanism with low percent ring substitution polystyrene resin. The objective is to show that the seven basic steps in heterogeneous catalysis are not adequate in explaining the mechanism of polymer-supported phase-transfer catalytic reactions. The major reason is that the two liquid solvents commonly used in phase-transfer reaction experiments are practically insoluble in each other. The solubility of toluene in water is 0.05 wt % and that of water in toluene is 0.03 wt % at 25 °C. Thus one must consider the consequence of having two immiscible liquid phases on the overall kinetics in more detail than the current view on the subject.[5] It will be shown here that the contacting times of the polymer particles with the respective aqueous and organic phases have a significant influence on the global kinetics, and these contacting times can be varied by adjusting the volume fractions of the two liquid phases.

The results are verified with the reaction of aqueous potassium cyanide with 1-bromooctane in toluene

$$n\text{-}C_8H_{17}Br + KCN_{aq} \rightarrow n\text{-}C_8H_{17}CN + KBr_{aq} \quad (1)$$

The reaction is catalyzed by polystyrene-bound benzyltri-*n*-butylphosphonium ions.[6] The polystyrene resins are microporous, cross-linked with 1% divinylbenzene, and have an effective 8.5% ring substitution.[7] To better illustrate our ideal, eq 1 is written as follows. The overall kinetic cycle[8] must be broken up into two steps by virtue of the presence of two practically insoluble liquid phases: an ion-exchange step in which the attached catalyst sites P^+ are in contact with the aqueous phase

$$P^+Br^-_s + K^+CN^-_{aq} \rightarrow P^+CN^-_s + K^+Br^-_{aq} \quad (2a)$$

and the chemical conversion step in which the active catalyst sites with cyanide ions react with the bromooctane in the organic solvent

$$P^+CN^-_s + n\text{-}C_8H_{17}Br_{org} \rightarrow P^+Br^-_s + n\text{-}C_8H_{17}CN_{org} \quad (2b)$$

The catalyst sites $P^+Br^-_s$ must be reactivated by ion-exchange step (2a) to provide the active form $P^+CN^-_s$. Hence we have to assess the immiscible liquid-phase effects *both*

0024-9297/86/2219-2435$01.50/0